Identification of a nonkinase target mediating cytotoxicity of novel kinase inhibitors

Petra Ross-Macdonald, Heshani de Silva, Qi Guo, Hong Xiao, Chen-Yi Hung, Becky Penhallow, Jay Markwalder, Liqi He, Ricardo M. Attar, Tai-an Lin, Steven Seitz, Charles Tilford, Judith Wardwell-Swanson, and Donald Jackson

Bristol-Myers Squibb Research and Development, Princeton, New Jersey

Abstract

In developing inhibitors of the LIM kinases, the initial lead molecules combined potent target inhibition with potent cytotoxic activity. However, as subsequent compounds were evaluated, the cytotoxic activity separated from inhibition of LIM kinases. A rapid determination of the cytotoxic mechanism and its molecular target was enabled by integrating data from two robust core technologies. High-content assays and gene expression profiling both indicated an effect on microtubule stability. Although the cytotoxic compounds are still kinase inhibitors, and their structures did not predict tubulin as an obvious target, these results provided the impetus to test their effects on microtubule polymerization directly. Unexpectedly, we confirmed tubulin itself as a molecular target of the cytotoxic kinase inhibitor compounds. This general approach to mechanism of action questions could be extended to larger data sets of quantified phenotypic and gene expression data. [Mol Cancer Ther 2008;7(11):3490–8]

Introduction

Protein kinase inhibitors represent an increasing class of cancer therapeutics. The approval of the BCR-ABL inhibitor imatinib for chronic myelogenous leukemia showed that an acceptable level of target specificity was achievable, and eight protein kinase inhibitors are now approved therapies for a variety of cancers (1). It is recognized that each drug has multiple activities; in some cases, this has been used to expand their indications. For example, imatinib has activities beyond BCR-ABL inhibition that allow efficacy in gastrointestinal stromal tumors (2). Studies of inhibitor specificity typically examine cross-reactivity against other protein kinases (3) or low-potency effects against target panels involved in liabilities (4). However, recent publications illustrate that kinase inhibitors are also capable of potent interactions that affect the function of additional protein classes (5–8). For example, an inhibitory activity of imatinib and nilotinib on the oxidoreductase enzyme Nqo2 has been shown; this activity is not shared with dasatinib (5, 7), a third kinase inhibitor approved in chronic myelogenous leukemia.

Clearly, it is preferable to characterize such off-target activities before approval of a therapeutic compound. However, identifying any additional molecular targets for a compound *de novo* remains challenging, especially in cases where small structural changes between compounds lead to large changes in activity (the ''activity cliff''; ref. 9). Mechanism of action projects have a high risk of failure and are associated with unpredictable timelines and specialized methods. Thus, compounds with unknown primary targets (or with evidence of an additional activity beyond a known primary target as in this case) are disfavored for development as drugs. Core technology platforms represent a new and attractive approach to molecular target identification. Studies can usually be initiated without a specific hypothesis or dedicated resources. For example, expression profiling (10–12) or high-content phenotypic assays (13, 14) have been used in recent reports of successful target identification.

We identified a series of potent inhibitors of the LIM kinases (LIMK). LIMK1 and LIMK2 regulate the actin cytoskeleton by phosphorylating and inactivating the cofilin family of actin-depolymerizing factors (15, 16); LIMK1 also acts to destabilize microtubules (17) and regulates cell motility, including tumor metastasis (18). The potent cytotoxic activity of early compounds seemed to validate LIMKs as oncology targets. However, later compounds in the same series showed that cytotoxicity was distinct from LIMK inhibition. Given the possible utility in oncology, the identity of the additional cytotoxic target was of immediate interest. Additional targets for kinase inhibitors are often assumed to be other protein kinases. In this case, we used a standard panel of high-content assays for apoptosis, combined with gene expression profiling, to rapidly gain insight on the mechanism. By coordinating the selection of test compounds, cellular model, timing, and dosing levels, these methods jointly identified the mechanism for cytotoxicity and suggested an appropriate biochemical assay to confirm direct inhibition of microtubule polymerization as the cytotoxic target, rather than a kinase. Identifying the most informative assays is the biggest hurdle in mechanism of action studies. Our approach of combining high-content assays with expression profiling could be extended to larger data sets of quantified phenotypic (14) and gene expression (10) data.

Received 4/24/08; revised 8/27/08; accepted 8/28/08.

The costs of publication of this article were defrayed in part by the payment of page charges. This article must therefore be hereby marked *advertisement* in accordance with 18 U.S.C. Section 1734 solely to indicate this fact.

Note: Current address for R.M. Attar: Ortho Biotech Oncology R&D/ Centocor R&D, Radnor, PA. Current address for T. Lin: Hoffmann-La Roche, Nutley, NJ.

Requests for reprints: Donald Jackson, Bristol-Myers Squibb Research and Development, P.O. Box 5400, Princeton, NJ 08543-5400. Phone: 609-818-5139; Fax: 609-818-6935. E-mail: donald.jackson@bms.com

doi:10.1158/1535-7163.MCT-08-0826

Materials and Methods

Source and Quality of Compounds

Compounds **1** to **6** were synthesized as described in the Supplementary Tables.[1] Compound purity was ≥97% as determined by reverse-phase high-performance liquid chromatography and proton nuclear magnetic resonance. Compound identities were confirmed by low-resolution mass spectrometry combined with ^{1}H, ^{19}F, and ^{13}C nuclear magnetic resonance spectrometry. Solvents and reagents were purchased from commercial sources and used without further purification. Nocodazole and paclitaxel were purchased commercially (Sigma-Aldrich). All compounds were resuspended in DMSO at 10 mmol/L (final) and diluted in culture medium before addition to cells.

In vitro LIMK Inhibition Assays

The protein kinase domains of human LIMK1 (accession no. P53667, amino acids 321-647) and LIMK2 (accession no. P53671, amino acids 312-638) were expressed as glutathione *S*-transferase fusion proteins using the Bac-to-Bac system (Invitrogen) in Sf9 cells. Compounds **1** to **6** were assayed for inhibition of LIMK1 and LIMK2 protein kinase activity by radioactive phosphate incorporation into biotinylated full-length human destrin (accession no. P60981). Reactions were done with a concentration series of compound in 25 mmol/L HEPES, 100 mmol/L NaCl, 5 mmol/L $MgCl_2$, 5 mmol/L $MnCl_2$, 1 μmol/L total ATP, 83 μg/mL biotinylated destrin, 167 ng/mL glutathione *S*-transferase-LIMK1, or 835 ng/mL glutathione *S*-transferase-LIMK2 in a total volume of 60 μL at room temperature for 30 min (LIMK1) or 60 min (LIMK2). Reactions were terminated by addition of 140 μL of 20% TCA/100 mmol/L sodium pyrophosphate, and the precipitates were harvested onto GF/C unifilter plates (PerkinElmer). The radioactivity incorporated was determined using a TopCount (Packard Instruments) after addition of 35 μL Microscint scintillation fluid (Perkin-Elmer).

Multiplexed High-Content Assay for Cell Count, DNA Content, Phospho-Histone H3, and α-Tubulin

A549 human lung cancer cells were seeded in collagen 1-coated black/clear 96-well assay plates (BD Biosciences) in RPMI 1640/5% fetal bovine serum (Cellgro) at 7,000 per well (for 2 h treatment) or 4,000 per well (for 24 h treatment) 16 h before treatment with vehicle or compounds (final 0.1% DMSO) for 2 or 24 h as indicated.

Following incubation, cells were fixed at room temperature with 2.3% formaldehyde (final), blocked in PBS with 0.25% Triton X-100 plus 2% bovine serum albumin, and stained with 6-diamidino-2-phenylindole (fluorescent channel 1), mouse anti-α-tubulin followed by Alexa 488 goat anti-mouse (Invitrogen; fluorescent channel 2) and Alexa 546-phalloidin (Invitrogen; fluorescent channel 3), and rabbit anti-phospho-histone H3 (Millipore/Upstate) followed by Alexa 647 goat anti-rabbit (Invitrogen; fluorescent channel 4). Images were obtained with a Cellomics Arrayscan using a ×10 objective with the XF93 (channels 1-3) and XF110 (channel 4) filter sets and analyzed using the Target Activation V2 Bioapplication (ThermoFisher Scientific). For α-tubulin measurements at 2 h, staining for phospho-histone H3 was used to exclude mitotic cells. No gating was used for 24 h measurements.

High-Content Phospho-Cofilin Assay

A549 cells were seeded at 3,000 per well in collagen 1-coated black/clear 96-well assay plates (BD Biosciences) in RPMI 1640/10% fetal bovine serum and incubated overnight. The medium was replaced with RPMI 1640/0.1% fetal bovine serum and cells were incubated an additional 24 h. The cells were then returned to RPMI 1640/10% fetal bovine serum and treated with compound or vehicle for 2 h (final 1% DMSO). Cells were fixed with 4% formaldehyde and stained with 6-diamidino-2-phenylindole (fluorescent channel 1) and rabbit anti-phospho-cofilin (Biosource) followed by Alexa 488 goat anti-rabbit IgG (Invitrogen; fluorescent channel 2). Images were obtained with a Cellomics Arrayscan using a ×10 objective with the XF100 filter set and analyzed using the Target Activation V2 Bioapplication (ThermoFisher Scientific).

Dose-Response Analysis of High-Content Assay Data

Results were normalized to the mean of the DMSO control data and plotted as individual data points. Curves were fit using GraphPad Prism (GraphPad Software).

Expression Profiling

Three biological replicate samples for each treatment were handled in separate blocks throughout. A549 cells were seeded at 50,000/cm^2 in RPMI 1640/10% fetal bovine serum (Cellgro) 16 h before treatment with vehicle or compounds (final 0.5% DMSO) for 7 h. RNA was prepared by manufacturer's protocols using the RNeasy Mini Kit (Qiagen; experiment 1) or the ABI 6100 (Applied Biosystems; experiment 2) followed by the RNAClean kit (Agencourt Bioscience) and evaluation of integrity on a Bioanalyzer 2100 (Agilent Technologies). Total RNA was processed for Human Genome U133A_2 (2.5 μg; experiment 1) or HT Human Genome U133A (1 μg; experiment 2) arrays and scanned with a GCS3000 (experiment 1) or a GeneChip HT scanner (experiment 2) using the manufacturer's protocols (Affymetrix). Background signal was defined as the highest intensity value observed for the AFFX_TrpnX probesets. The ArrayExpress identifier for these data is E-TABM-450.

Tubulin Polymerization Assay

Compounds at 2 mmol/L in DMSO were diluted to 100 μmol/L in assay buffer [80 mmol/L sodium PIPES (pH 6.9), 1 mmol/L $MgCl_2$, 1 mmol/L EGTA]. One-tenth volume was added to assay buffer containing 4.5 mg/mL purified bovine neuronal tubulin (Cytoskeleton) 15% glycerol (v/v) and 2 mmol/L GTP on ice. Reaction mixes were transferred to 37°C, and absorbance at 340 nm was measured for 60 min at 1 min intervals preceded by 5 s of orbital shaking using a Spectramax Plus spectrophotometer (Molecular Devices).

Statistical Analysis

Principal component analysis of high-content assay data was done using a correlation matrix with normalized eigenvector scaling in Genomics Suite 6.2 (Partek). For

[1] Supplementary data for this article are available at Molecular Cancer Therapeutics Online (http://mct.aacrjournals.org/).

expression profiling data, both two-way ANOVA analyses and paired *t* tests (two-tailed) using handling block as a random factor were done on the variance stabilization normalization intensity values (19) for each treatment and the vehicle control using the ANOVA and step-up false discovery rate functions in Genomics Suite 6.2 (Partek). The general conclusions from ANOVA and *t* test analyses were identical; results from the *t* test analysis are presented because they are independent of other treatment data. For the false discovery rate calculation, only probesets for which at least two samples showed signal above negative controls were included (20930 for experiment 1 and 20479 for experiment 2). To select lists for enrichment analysis, we used the recommendations of the MicroArray Quality Control Consortium (20): for each treatment, the probesets with $P \leq 0.01$ were ranked in order of absolute fold change (mean of 3 replicates). We then calculated the odds for the observed representation of each Gene Ontology (GO) category in sublists taken incrementally from this ranked set based on the hypergeometric distribution of *i, n, m*, and *N* (where *i* is the number in the sublist that matches a GO category, *n* is the number on the array that matches a GO category, *m* is = the number on the array that does not match a GO category, and *N* is the number of probesets in the sublist). The lowest *P* value obtained from all sublists is presented and contains a Bonferroni correction for both the number of probesets in the sublist and the number assigned to the GO category.

Compound Comparisons

Compound similarity scores were calculated as Tanimoto scores with the ECFP_4 descriptor set using Pipeline

Table 1. Structure and properties of compounds tested

Compound	1	2	3	4	5	6
Class	Dual	Dual	LIMKi	LIMKi	Cytotoxic	Cytotoxic
R1	EtO	Cyclopropyl	Isopropyl	N/A	MeO	MeO
R2	CHF_2	CHF_2	CHF_2	N/A	CHF_2	H
R3	Cl	Cl	Cl	N/A	H	H
R4	Cl	Cl	Cl	N/A	H	H
R5	H	H	H	N/A	CH_3	CH_3
R6	H	H	H	N/A	CH_3	CH_3
LIMK1 IC_{50} (nmol/L)*	55	5	7	22	334	769
LIMK2 IC_{50} (nmol/L)*	51	6	8	14	3,125	3,125
A549 EC_{50} (nmol/L)†	69	154	>10,000	>50,000	7	<68
Dose for profiling (nmol/L)	30	30	1,000	1,000	2, 4, 8	2, 4, 8

Structural comparison‡

Compound	1	2	3	4	5	6
1	1.00	**0.69**	**0.74**	0.25	**0.56**	**0.38**
2	**0.69**	1.00	**0.74**	0.20	**0.49**	**0.32**
3	**0.74**	**0.74**	1.00	0.22	**0.52**	**0.34**
4	0.25	0.20	0.22	1.00	0.27	**0.30**
5	**0.56**	**0.49**	**0.52**	0.27	1.00	**0.66**
6	**0.38**	**0.32**	**0.34**	**0.30**	**0.66**	1.00
Nocodazole	0.17	0.14	0.15	0.16	0.22	0.24
Paclitaxel	0.08	0.08	0.08	0.07	0.08	0.08
Colchicine	0.09	0.11	0.08	0.12	0.11	0.11
Vinblastine	0.08	0.07	0.06	0.08	0.07	0.08

**In vitro* assay for kinase activity on human destrin substrate.
†Proliferation of A549 cells measured by [^{3}H]thymidine incorporation (**1**, **4**, **5**, and **6**) or colony formation (**2-4**).
‡Tanimoto similarity using ECFP_4 descriptor set. Values ≥ 0.3 are indicated in bold.

Compounds 1, 2, 3, 5, 6

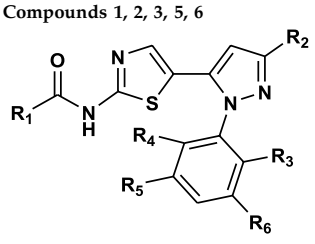

Compound 4

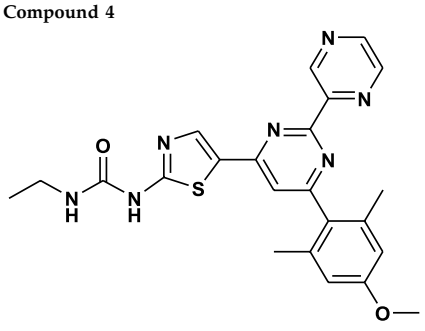

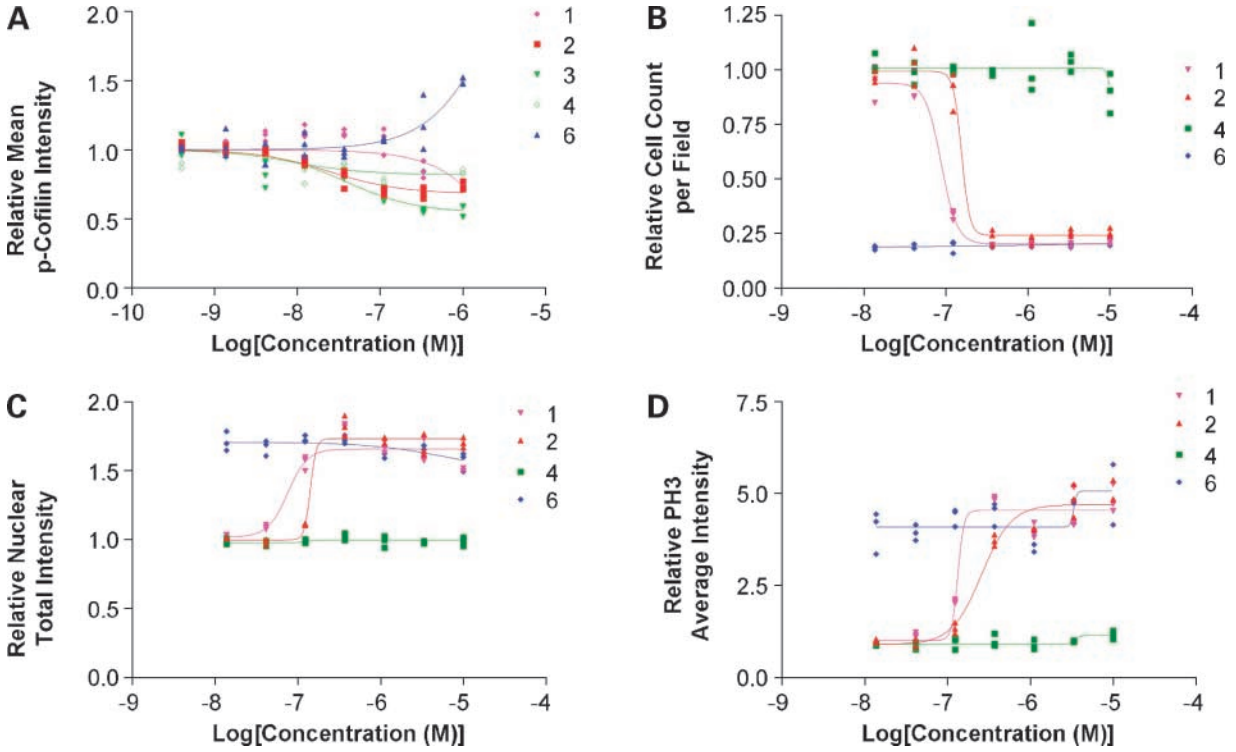

Figure 1. Effect of compounds on cellular phenotypes. A549 cells were treated with dual compounds **1** and **2**, LIMKi compound **4**, and cytotoxic compound **6** at concentrations from 1 to 0.0014 μmol/L (**A**) or from 10 to 0.014 μmol/L (**B** and **D**) as a 3-fold dilution series and measured by high content assays. **A,** phosphorylated cofilin after 2 h treatment. **B,** cell count after 24 h treatment. **C,** total nuclear DNA intensity after 24 h treatment. **D,** phospho-histone H3 after 24 h treatment. Values were normalized to the mean of 0.1% DMSO-treated control data; markers show data points for each of the three replicates.

Pilot 6.1 (Scitegic/Accelerys). Structures for nocodazole, paclitaxel, colchicine, and vinblastine were obtained as SMILES strings from the PubChem database.[2] Kinase inhibitor compounds from the WOMBAT (Sunset Molecular Discovery) and AurSCOPE Kinase (Aureus-Pharma) databases were selected by querying for K_i, EC_{50}, or IC_{50} values of ≤10 μmol/L for any protein assigned to GO classification 0004672 (protein kinase activity). Compounds inhibiting more than 20 targets by these criteria were excluded from analysis.

Results

Identification of an Off-Target Activity in a Series of Kinase Inhibitors

Within a series of kinase inhibitors, early compounds such as **1** and **2** inhibited LIMK activity *in vitro* and affected cell proliferation and survival *in vivo* (Table 1). However, some later compounds showed either LIMK inhibition (e.g., compound **3**) or proliferation and survival effects (e.g., compounds **5** and **6**). A structurally distinct compound, **4**, also inhibited LIMKs *in vitro* but did not affect cell survival or proliferation. These observations suggested that the cytotoxic activity of early compounds resulted from a second target unrelated to LIMK inhibition and led us to classify **1** and **2** as ''dual'' (having both cytotoxic and LIMK activities), **3** and **4** as ''LIMKi'' (noncytotoxic LIMK inhibitors), and **5** and **6** as ''cytotoxic'' (having cytotoxic activity but no LIMK activity). Like the dual compounds **1** and **2**, the LIMKi **3** and **4** inhibited phosphorylation of the LIMK substrate cofilin in a cellular assay (Fig. 1A), showing that their lack of cytotoxicity was not due to lack of uptake; the apparent increase in phospho-cofilin intensity for **6** is caused by mitotic cell rounding. Binding assays (21) on a panel of 41 kinases (compounds **5** and **6**) or 287 kinases (compounds **2-4**) indicated that both cytotoxic and dual compounds retain the ability to inhibit protein kinases. However, no shared target was identified in the 41 protein kinases tested with dual compound **2** and cytotoxic compounds **5** and **6** (see Supplementary Table S1)[1].

High-Content Assays Indicate an Effect on Microtubule Stability

We tested compounds from all three classes for effects on proliferation and survival in A549 human lung cancer cells using our standard panel of high-content assays for cell count, nuclear DNA content, histone H3 phosphorylation, and α-tubulin intensity (Fig. 1). The dual compounds **1** and **2** caused a dose-dependent reduction in cell count (Fig. 1B) and induced mitotic arrest as shown by increases in total nuclear DNA intensity (Fig. 1C) and histone H3

[2] pubchem.ncbi.nlm.nih.gov

phosphorylation (Fig. 1D) after 24 h treatment. Cytotoxic **6** proved highly potent, causing similar effects even at the lowest dose tested of 14 nmol/L. A dose-dependent increase of caspase-3 activation was seen after 24 h of treatment with **1**, **5**, or **6** (data not shown), showing that the reduction in cell count results from a combination of increased apoptosis and decreased proliferation. By contrast, LIMKi **4** had no effect on these variables even at the highest dose tested.

Our high-content assay panel included α-tubulin immunofluorescence as an indicator of cell rounding in mitosis or apoptosis. However, we observed a distinctive and potent effect for the cytotoxic and dual compounds on this measurement (Fig. 2). Cytotoxic **6** reduced the intensity of localized α-tubulin staining in the majority of cells after 2 h (Fig. 2B). By contrast, LIMKi **3** treatment was indistinguishable from the control treatment even at the highest dose tested (Fig. 2C). The effects of the dual compounds **1** and **2** resembled those of cytotoxic compound **6** (Fig. 2D) and are similar to treatment with the known cytotoxic microtubule-destabilizing agent nocodazole (13).

The overall similarity between phenotypic effects of our inhibitors and those of nocodazole was identified and quantified by principal component analysis of data from 30 cytologic features drawn from several distinct high-content assays (Fig. 3; Supplementary Table S2).[1] These features reflect nuclear morphology, DNA content, apoptosis induction, microtubules, actin filaments, and cofilin phosphorylation. Our cytotoxic compounds (compounds **1**, **5**, and **6**) nocodazole and paclitaxel all showed dose-dependent separation from LIMKi **3** and the DMSO control in principal component 1, and dual compound **1** and cytotoxics **5** and **6** grouped with nocodazole rather than paclitaxel in principal component 2.

Expression Profiling Indicates an Effect on Microtubule Stability

Our studies on the effects of the compounds on gene expression were guided by early results from high-content assays for cell count and cofilin phosphorylation (Fig. 1). A treatment of only 7 h was chosen to precede apoptosis, whereas dose levels (see Table 1) captured both cytotoxic

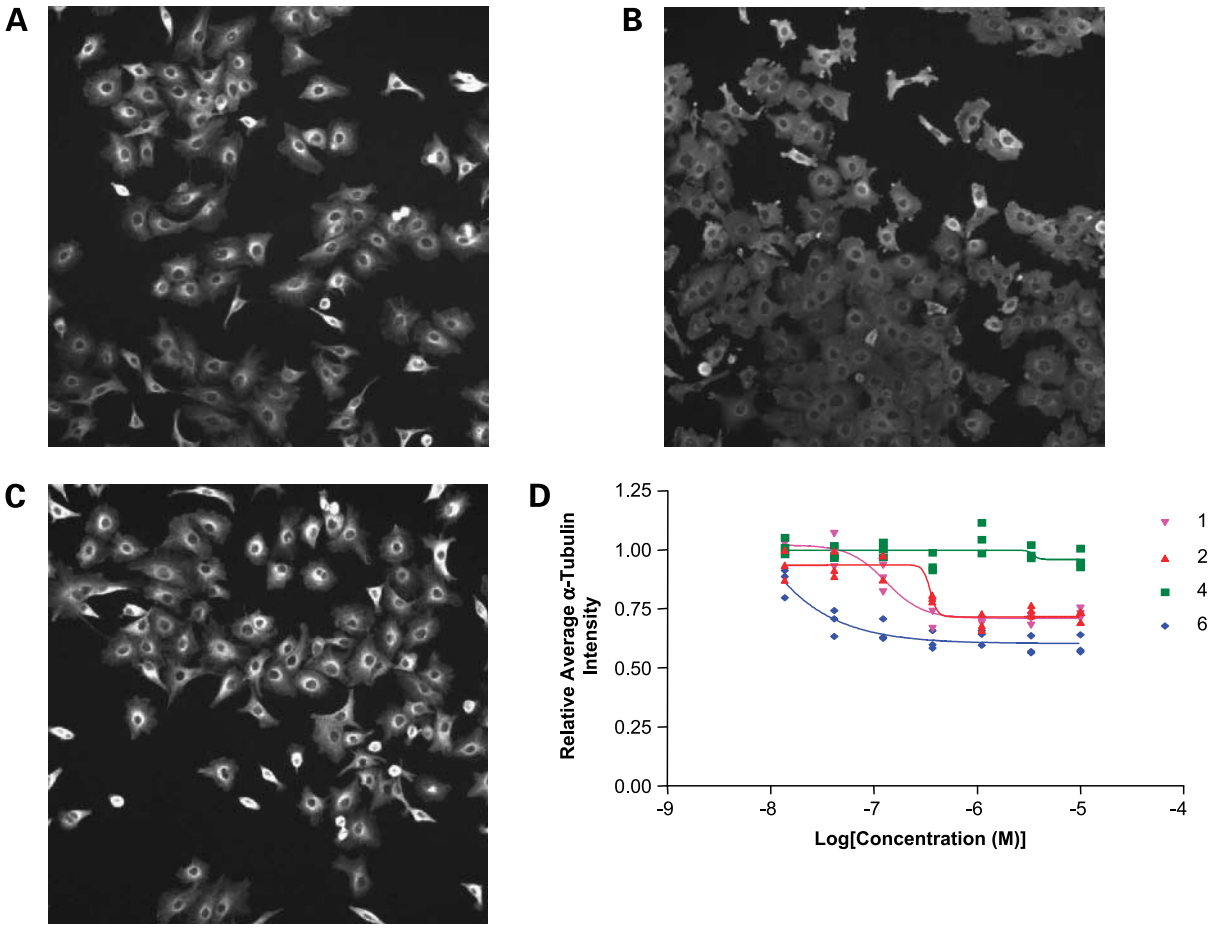

Figure 2. Effect of compounds on α-tubulin localization. A549 cells were treated for 2 h with (**A**) 0.1% DMSO, (**B**) 10 μmol/L compound **6**, or (**C**) 10 μmol/L compound **4**. **D,** average α-tubulin staining intensity (relative to DMSO control) for the nonmitotic cells in A549 cultures treated with compounds **1, 2, 4**, and **6** for 2 h at concentrations from 10 to 0.0014 μmol/L as a 3-fold dilution series. Values were normalized to the mean of 0.1% DMSO-treated control wells; markers show data points for each of the three replicates.

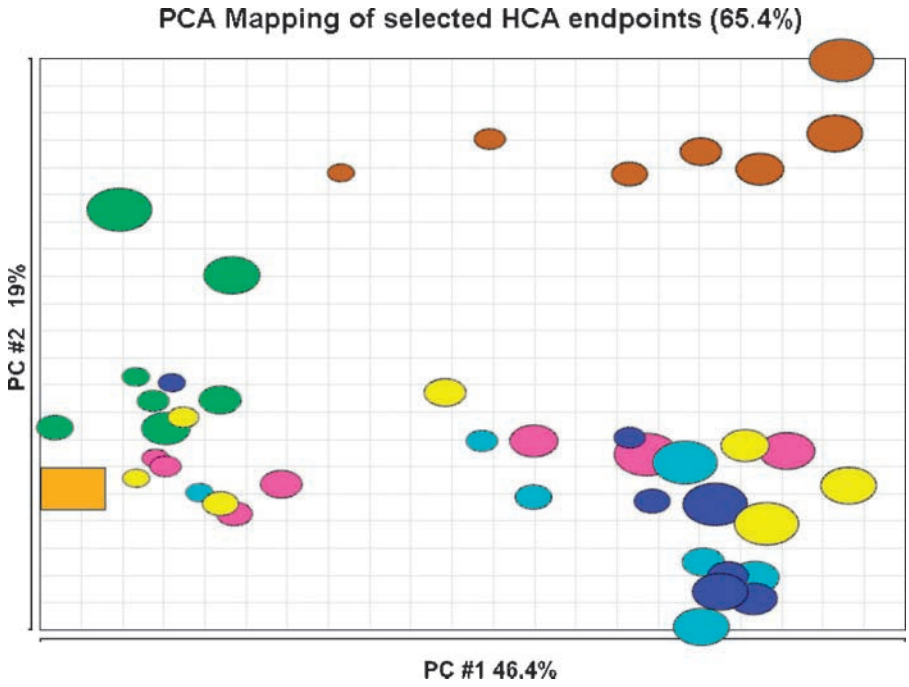

Figure 3. Principal component analysis of quantitative phenotypic data. Thirty measurements drawn from several distinct high-content assays were used. Data were obtained in A549 cells treated for 2 and 24 h with 0.1% DMSO (*orange square*), compound **1** (*magenta*), **3** (*green*), **5** (*cyan*), **6** (*blue*), paclitaxel (*brown*), or nocodazole (*yellow*) at seven concentrations from 10 to 0.014 μmol/L as a 3-fold dilution series. Larger markers indicate higher doses. Original variables and component loadings are listed in Supplementary Table S2.

activity and cellular inhibition of LIMK for the dual compounds **1** and **2**, captured LIMK inhibition for compounds **3** and **4**, and captured cytotoxicity for compounds **5** and **6** and nocodazole. The cytotoxic treatments (compounds **1**, **2**, **5**, and **6** and nocodazole) had a very limited effect on transcript levels, with only a few genes identified as differentially regulated (Fig. 4A; see Supplementary Table 3[1] for all *P* values and fold-change). However, a striking predominance of tubulin subunit genes was noted. A statistical analysis confirmed that genes assigned to GO (22) categories involving microtubules were significantly overrepresented in the transcripts affected by three compounds with cytotoxic activity (compounds **2**, **5**, and **6**). This category was also overrepresented for nocodazole (Fig. 4B). The level of certain tubulin subunit mRNAs is known to be directly regulated by unpolymerized tubulin subunits (23). The Affymetrix array contains probesets for 17 tubulin subunits; a dose-related decrease in signal for up to eight of these was seen with the dual (**1** and **2**) and cytotoxic (**5** and **6**) compounds and nocodazole but not with the LIMKi compounds **3** and **4** (Fig. 4C). Thus, all compounds with cytotoxic activity (compounds **1**, **2**, **5**, and **6** and nocodazole) reduced the levels of tubulin transcripts (although the data for dual compound **1** did not meet strict criteria for significance in this treatment).

Our mRNA expression profiling did not suggest any additional sources of cytotoxic activity for the compounds at the doses used. For our three compounds with cytotoxic activity in profiling experiment 2 (compounds **2**, **5**, and **6**), there were nine shared probesets that met the criteria of >1.2-fold change, 20% false discovery rate (Fig. 4A); all correspond to tubulin subunits. Within the relaxed significance limit of $P < 0.01$ used to select probesets for enrichment analysis (Fig. 4B), only 13 probesets were affected by all three compounds, and all correspond to tubulin subunits.

Cytotoxic Compounds Inhibit Tubulin Polymerization *In vitro*

To determine whether the cytotoxic and dual compounds act directly on tubulin subunits, we performed *in vitro* tubulin polymerization assays using purified components (Fig. 5). Relative to the vehicle control, addition of 10 μmol/L paclitaxel accelerated formation of microtubules, whereas 10 μmol/L nocodazole decreased both the rate and the overall level of microtubule formation. Addition of either 10 μmol/L **2** (dual) or 10 μmol/L **5** (cytotoxic) also decreased the rate and level of microtubule polymerization. Both compounds caused greater inhibition than the known microtubule-depolymerizing agent nocodazole. By contrast, LIMKi **3** had no effect on the rate of signal increase and little or no effect on the final levels. Thus, the cytotoxic and dual compounds act directly on tubulin subunits to affect their polymerization.

Effects on Tubulin Are Not Predicted by Structural Analysis

We performed comparisons of our compound series and known microtubule-destabilizing agents using a circular molecular fingerprint (see Materials and Methods). The highest Tanimoto similarity was 0.24 for cytotoxic **6** versus nocodazole (Table 1). The initial lead compounds **1** and **2**, which are potent inhibitors of both LIMK activity and tubulin polymerization, have even lower similarity scores, equivalent to those of the noncytotoxic LIMKi **3** and **4**. Although the Tanimoto scores for similarity to colchicine were ≤0.12 (Table 1), in a retrospective visual inspection of the series, a similarity to the colchicine pharmacophore (24) was noted. Comparison of nocodazole to 8,477 reported kinase inhibitors from WOMBAT and AUREUS databases identified 168

compounds with Tanimoto scores that were higher than the 0.24 similarity score for compound **6** (Supplementary Table S4).[1] Two of the 168 compounds (a cyclin-dependent kinase inhibitor and a LCK inhibitor) had Tanimoto scores greater than 0.4 against nocodazole, suggesting that microtubule-depolymerizing activity exists in additional chemical series of kinase inhibitors.

Discussion

Having established that the cytotoxicity of early lead compounds resulted from activity on a second target unrelated to their potent LIMK inhibition, we used cell-based core technology platforms to determine that such compounds act to destabilize microtubules. High-content assays showed that loss of localized α-tubulin immunofluorescence in cells treated with dual activity or cytotoxic compounds coincides with the induction of mitotic arrest and reduction in cell number. An unsupervised analysis of the phenotypic data showed clustering with the microtubule destabilizer nocodazole. Expression profiling showed that the only consistent changes observed across treatments with both cytotoxic and dual activity compounds were significant reductions in tubulin subunit

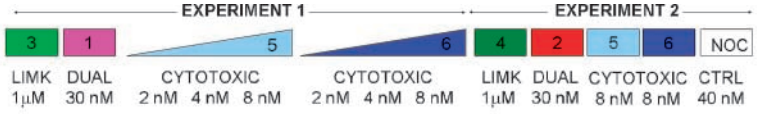

A

Meet 20% FDR and 1.2-fold change	0	0	0	0	5	0	0	0	278	11	20	9	1
Subset annotated to Tubulin gene					4				2	11	20	9	1

B

Meet P < 0.01; submitted to EA	213	65	35	74	560	24	21	50	1262	363	234	454	161
Number of these probesets in GO:0046785				3	12					13	22	13	9
p value for enrichment of GO:0046785	> 0.05	> 0.05	> 0.05	3.8 E-05	3.7 E-26	> 0.05	> 0.05	> 0.05	> 0.05	1.2 E-30	1.7 E-53	1.3 E-30	5.9 E-17

C

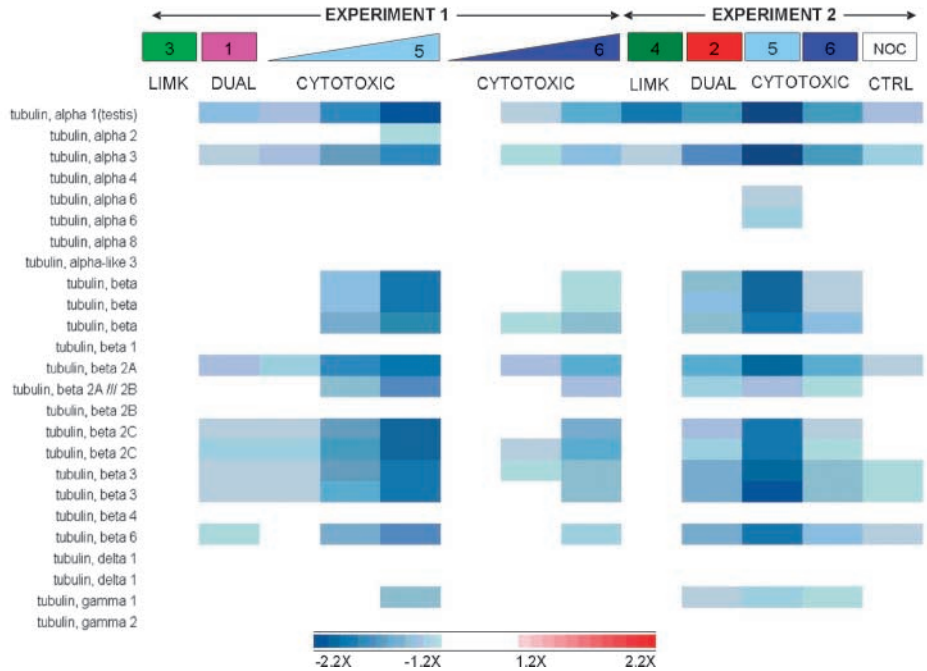

Figure 4. Effect of compounds on microtubule-related transcripts and enrichment of the GO term for microtubule polymerization. **A,** number of probesets meeting criteria of 1.2-fold change from vehicle control with a false discovery rate of 10% and representation of tubulin genes therein. **B,** probesets meeting $P < 0.01$ for change in expression relative to vehicle control were rank-ordered by absolute fold change relative to vehicle control and submitted to enrichment analysis (*EA*). The GO biological process category ''0046785: Microtubule polymerization'' containing 39 probesets was ranked highest for cytotoxic compounds **2, 5**, and **6**. The number of probesets submitted, the *P* value for enrichment of category 0046785, and the representation of its 39 probe sets in the treatment lists with significant enrichment are shown. **C,** for the 25 probesets annotated to represent 17 tubulin genes on the HU133A array series, the mean fold change from vehicle control is shown. Expression changes of >1.2-fold appear in color that saturates at 2.2-fold change.

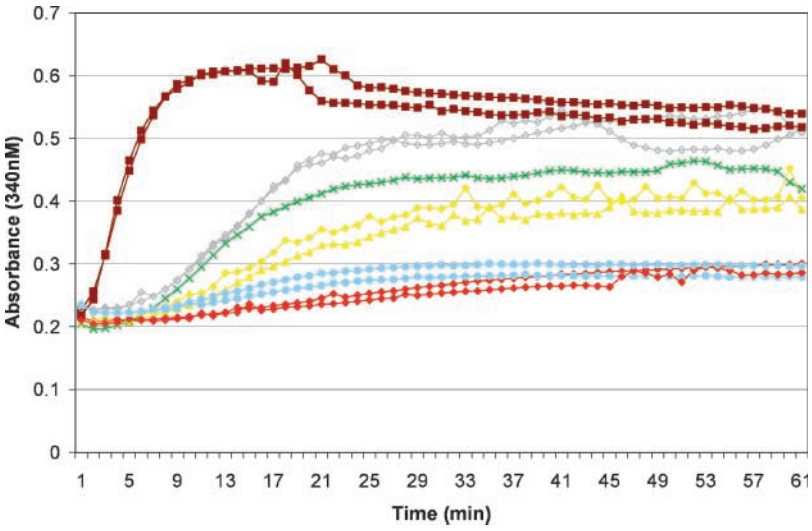

Figure 5. Effect of compounds on tubulin polymerization *in vitro*. Dual compound **2** (*red diamonds*), LIMKi compound **3** (*green crosses*), and cytotoxic compound **5** (*light blue circles*), paclitaxel (*brown squares*), and nocodazole (*yellow triangles*) were tested for effects on polymerization of purified bovine brain tubulin and quantified by absorbance at 340 nm. All compounds were tested at 10 μmol/L in 0.5% DMSO. *Gray open diamonds,* a control treatment with vehicle. Each curve represents an individual experimental sample; two independent samples are shown for all compounds, except compound **3**.

mRNAs. This rapid and highly specific effect also pointed to microtubule depolymerization, which is known to cause post-transcriptional destabilization of tubulin subunit transcripts (25). Although others have implicated LIMK1 in control of microtubules (17), their work predicts that LIMK inhibition would stabilize microtubules. Finally, we showed that dual compound **2** and cytotoxic compounds **5** directly depolymerize microtubules *in vitro*, but the closely related LIMKi compound **3** does not. The direct effect on tubulin polymerization *in vitro* is sufficient to explain the activity of cytotoxic and dual compounds, because known depolymerizing agents such as nocodazole are cytotoxic (26).

It is commonly assumed that additional targets of kinase inhibitors will be kinases or at least ATP-binding proteins. However, there are recent reports of potent and specific interactions between kinase inhibitors and a G-protein-coupled receptor (6) and with two nicotinamide-dependent oxidoreductases (5, 7, 8). Demonstration of the GTPase tubulin as a third novel target highlights our incomplete understanding of this therapeutic class. Microtubule activity was not anticipated in our compound series or predicted by a routine structural comparison.

Measuring structure/activity relationships at the cellular level is receiving increasing attention. A recent analysis of >6,000 diverse compounds using high-content assays similar to ours noted that 4% of compounds with Tanimoto similarity of ≥0.3 show discordant phenotypes (14). Combining multiple approaches might indicate off-target activities that are not evaluated through typical *in vitro* selectivity screens, which typically incorporate only other kinases (21) and enzymes or receptors that mediate clinical liabilities.

Compounds with unknown targets are disfavored for development as drugs and have limited utility as experimental probes of cellular function. Off-target activity may affect the development of a drug in several ways. For example, identification of an additional, proapoptotic target for a class of farnesyl transferase inhibitors had implications for both efficacy and toxicity (27). However, it is not always obvious that an observed effect of a compound is not mediated by the intended target. This is especially difficult with oncology compounds, where growth inhibition is often a primary assay. In the present case, the potent cytotoxicity of early compounds was noted because although LIMKs regulate tumor cell invasion and proliferation (28, 29), neither kinase had been identified as essential for cell survival. However, only the divergence of LIMK inhibition and cytotoxicity that was revealed by later compounds confirmed that a second target existed. Once off-target activity has been recognized, it remains to identify the unknown molecular target. There is no clear best practice for this (30), and published examples of success are rare (31). Analyses of kinase inhibitor selectivity often focus on selectivity versus other protein kinases (32) and methods are available to test this (3). Our findings and others (6, 7) show that additional, non-ATP-dependent proteins may also mediate off-target effects of kinase inhibitors.

We have shown that combining two cell-based platforms (high-content assays and mRNA expression profiling) provides a powerful system for identifying and guiding the analysis of off-target activities. A potential mechanism need not be hypothesized in advance, and specific confirmatory assays can be selected based on the results. High-content assays enable rapid, low-cost examination of many compounds in phenotypic assays such cell cycle progression (14) combined with mechanistic assays such as phosphorylation of a kinase substrate (33). By contrast, expression profiling provides a broad measure of cellular state without needing a physiologic endpoint and facilitates comparison with previous data (10). In this work, results from routine high-content assays directed the design of expression profiling studies; in other cases, expression profiling results could suggest mechanistic endpoints for confirmation in high-content assays. In either case, coordinated selection of test compounds, cellular model, timing, and dosing levels simplifies interpretation of the combined result set. Our success illustrates that combining information from generic assays can identify the specific and labor-intensive assays that ultimately confirm the target.

Disclosure of Potential Conflicts of Interest

All authors are current or former employees of Bristol-Myers Squibb.

Acknowledgments

We thank the B-MS Expression Technologies Group and Isaac Neuhaus for generating and handling array data, Myles Fennell for providing feedback on the article, and Mark Cockett and George Trainor for providing invaluable support for this work.

Author contributions: Q. Guo, H. Xiao, J. Wardwell-Swanson, and D. Jackson developed, performed, and analyzed the high-content assays. H. de Silva and P. Ross-Macdonald performed and analyzed the mRNA expression profiling treatments. C. Tilford and H. de Silva performed the GO category analysis. D. Jackson and C. Tilford performed the compound similarity analyses. J. Markwalder, L. He, and S. Seitz synthesized the novel compounds. B. Penhallow, C-Y. Hung, and T. Lin performed the initial *in vitro* and cellular assays that classified the compounds. B. Penhallow and R.M. Attar performed the *in vitro* tubulin polymerization assay. P. Ross-Macdonald and D. Jackson jointly prepared this article.

References

1. Giamas G, Stebbing J, Vorgias CE, Knippschild U. Protein kinases as targets for cancer treatment. Pharmacogenomics 2007;8:1005 – 16.

2. Baselga J. Targeting tyrosine kinases in cancer: the second wave. Science 2006;312:1175 – 8.

3. Karaman MW, Herrgard S, Treiber DK, et al. A quantitative analysis of kinase inhibitor selectivity. Nat Biotechnol 2008;26:127 – 32.

4. Paolini GV, Shapland RHB, van Hoorn WP, Mason JS, Hopkins AL. Global mapping of pharmacological space. Nat Biotechnol 2006;24: 805 – 15.

5. Bantscheff M, Eberhard D, Abraham Y, et al. Quantitative chemical proteomics reveals mechanisms of action of clinical ABL kinase inhibitors. Nat Biotechnol 2007;25:1035 – 44.

6. Morel C, Ibarz G, Oiry C, et al. Cross-interactions of two p38 mitogen-activated protein (MAP) kinase inhibitors and two cholecystokinin (CCK) receptor antagonists with the CCK1 receptor and p38 MAP kinase. J Biol Chem 2005;280:21384 – 93.

7. Rix U, Hantschel O, Durnberger G, et al. Chemical proteomic profiles of the BCR-ABL inhibitors imatinib, nilotinib, and dasatinib reveal novel kinase and nonkinase targets. Blood 2007;110:4055 – 63.

8. Tanaka M, Bateman R, Rauh D, et al. An unbiased cell morphology-based screen for new, biologically active small molecules. PLoS Biol 2005; 3:e128.

9. Maggiora GM. On outliers and activity cliffs—why QSAR often disappoints. J Chem Inf Model 2006;46:1535 – .

10. Lamb J, Crawford ED, Peck D, et al. The Connectivity Map: using gene-expression signatures to connect small molecules, genes, and disease. Science 2006;313:1929 – 35.

11. Luesch H, Chanda SK, Raya RM, et al. A functional genomics approach to the mode of action of apratoxin A. Nat Chem Biol 2006;2: 158 – 67.

12. Wei G, Twomey D, Lamb J, et al. Gene expression-based chemical genomics identifies rapamycin as a modulator of MCL1 and glucocorticoid resistance. Cancer Cell 2006;10:331 – 42.

13. Barabasz A, Foley B, Otto JC, Scott A, Rice J. The use of high-content screening for the discovery and characterization of compounds that modulate mitotic index and cell cycle progression by differing mechanisms of action. Assay Drug Dev Technol 2006;4:153 – 63.

14. Young DW, Bender A, Hoyt J, et al. Integrating high-content screening and ligand-target prediction to identify mechanism of action. Nat Chem Biol 2008;4:59 – 68.

15. Arber S, Barbayannis FA, Hanser H, et al. Regulation of actin dynamics through phosphorylation of cofilin by LIM-kinase. Nature 1998;393:805 – 9.

16. Yang N, Higuchi O, Ohashi K, et al. Cofilin phosphorylation by LIM-kinase 1 and its role in Rac-mediated actin reorganization. Nature 1998; 393:809 – 12.

17. Gorovoy M, Niu J, Bernard O, et al. LIM kinase 1 coordinates microtubule stability and actin polymerization in human endothelial cells. J Biol Chem 2005;280:26533 – 42.

18. Wang W, Eddy R, Condeelis J. The cofilin pathway in breast cancer invasion and metastasis. Nat Rev Cancer 2007;7:429 – 40.

19. Huber W, von Heydebreck A, Sueltmann H, Poustka A, Vingron M. Parameter estimation for the calibration and variance stabilization of microarray data. Stat Appl Genet Mol Biol 2003;2; Article 3.

20. The MicroArray Quality Control (MAQC) project shows inter- and intraplatform reproducibility of gene expression measurements. Nat Biotechnol 2006;24:1151 – 61.

21. Fabian MA, Biggs WH III, Treiber DK, et al. A small molecule-kinase interaction map for clinical kinase inhibitors. Nat Biotechnol 2005;23: 329 – 36.

22. Ashburner M, Ball CA, Blake JA, et al. Gene Ontology: tool for the unification of biology. Nat Genet 2000;25:25 – 9.

23. Cleveland DW, Lopata MA, Sherline P, Kirschner MW. Unpolymerized tubulin modulates the level of tubulin mRNAs. Cell 1981;25:537 – 46.

24. Nguyen TL, McGrath C, Hermone AR, et al. A common pharmacophore for a diverse set of colchicine site inhibitors using a structure-based approach. J Med Chem 2005;48:6107 – 16.

25. Cleveland DW, Havercroft JC. Is apparent autoregulatory control of tubulin synthesis nontranscriptionally regulated? J Cell Biol 1983;97: 919 – 24.

26. Mollinedo F, Gajate C. Microtubules, microtubule-interfering agents and apoptosis. Apoptosis 2003;8:413 – 50.

27. Lackner MR, Kindt RM, Carroll PM, et al. Chemical genetics identifies Rab geranylgeranyl transferase as an apoptotic target of farnesyl transferase inhibitors. Cancer Cell 2005;7:325 – 36.

28. Davila M, Frost AR, Grizzle WE, Chakrabarti R. LIM kinase 1 is essential for the invasive growth of prostate epithelial cells: implications in prostate cancer. J Biol Chem 2003;278:36868 – 75.

29. Amano T, Kaji N, Ohashi K, Mizuno K. Mitosis-specific activation of LIM motif-containing protein kinase and roles of cofilin phosphorylation and dephosphorylation in mitosis. J Biol Chem 2002;277:22093 – 102.

30. Terstappen GC, Schlupen C, Raggiaschi R, Gaviraghi G. Target deconvolution strategies in drug discovery. Nat Rev Drug Discov 2007;6: 891 – 903.

31. Burdine L, Kodadek T. Target identification in chemical genetics: the (often) missing link. Chem Biol 2004;11:593 – 7.

32. Vieth M, Higgs RE, Robertson DH, Shapiro M, Gragg EA, Hemmerle H. Kinomics-structural biology and chemogenomics of kinase inhibitors and targets. Biochim Biophys Acta 2004;1697:243 – 57.

33. Perlman ZE, Slack MD, Feng Y, Mitchison TJ, Wu LF, Altschuler SJ. Multidimensional drug profiling by automated microscopy. Science 2004; 306:1194 – 8.